Unravelling the Implications of Macromolecular Orientation on the Planer and Vertical Charge Transport in Organic Electronic Devices

Shubham Sharma[1*], Ajendra Kumar Vats[2], Manish Pandey[2*], Shuichi Nagamatsu[3], Jyh-Chien Chen[4], and Shyam S. Pandey[1*]

[1]Graduate School of Life Science and Systems Engineering, Kyushu Institute of Technology, 2-4 Hibikino, Wakamatsu, Kitakyushu 808-0196, Japan

[2]Division of Materials Science, Nara Institute of Science and Technology, Ikoma, Nara 630-0192, Japan

[3]Department of Computer Science and Electronics, Kyushu Institute of Technology, 680-4 Kawazu, Iizuka, 820-8502, Japan

[4]National Taiwan University of Science and Technology, No. 43, Section 4, Keelung Rd, Da'an District, Taipei City, 106, Taiwan

*Corresponding Author

S.S: shubhammudgal95@gmail.com; M.P: mpandey@ms.naist.jp; S.S.P: shyam@life.kyutech.ac.jp

ABSTRACT

The role of film morphology of conjugated polymers (CPs) and their macromolecular conformation with respect to substrate in governing charge transport and overall device performances has been a matter of debate. The nature of the macromolecular orientation of CPs in thin films plays a pivotal role in controlling the performance of planer and sandwich devices. Thin film characterizations unveiled that spin-coated films are isotropic with mixed edge-on/face-on conformation, whereas unidirectional floating film transfer method (UFTM) films are anisotropic with edge-on oriented micrometer-sized ordered domains. To unravel the explicit role of molecular orientation on device performance, two types

of devices, organic Schottky diodes (OSDs) for out-of-plane carrier transport and organic field-effect transistor (OFETs) for in-plane charge transport, were fabricated and characterized. Isotropic and relatively low crystalline spin-coated films exhibited superior transport characteristics in out-of-plane direction than UFTM films irrespective of the crystallinity. On the other hand, edge-on oriented UFTM thin films demonstrated remarkably enhanced in-plane charge transport with more than two orders of magnitude of enhancement in the field-effect mobility. The nature of molecular orientation of different films is well correlated with the performance of the OSDs and OFETs.

KEYWORDS: semiconducting polymers, floating-film transfer method, orientation, organic schottky diodes, organic field-effect transistors

1. INTRODUCTION

Solution processable conjugated polymers (CPs) have emerged as excellent organic semiconducting materials for various applications in the rapidly developing field of organic electronics. The optoelectronic properties of CPs can be easily tuned due to their inherent molecular self-assembly tendency.[1–4] Charge carrier transport in the CPs is dictated by the high-speed intrachain carrier motion along the π-conjugated polymeric backbone followed by interchain hopping in the π–π stacking direction.[5–7] It has been widely accepted in the material science community that charge-carrier transport in CPs stringently depends on their film crystallinity.[8–11] Improving the crystallinity of thin films of CPs results in high field-effect carrier mobility in planar devices like organic field-effect transistors (OFETs) as well as out-of-plane mobility in vertical (sandwich) devices like organic solar cells and organic Schottky diodes (OSDs).[8–15] Moreover, the molecular orientation of the CPs with respect to the substrate

plane is crucial for the efficient charge transport in the direction of the electrode for a device architecture under investigation.[13,16] In general, there exists three types of molecular orientations that CPs adopt in thin films: edge-on, face-on, and end-on. Depending on the device geometry, efforts have been directed to optimize the orientation of CPs in their thin films to improve device performances.[13,16–19] It has been well established that edge-on orientation of the polymers in their thin films are important for a planar device such as OFETs due to the presence of both conjugated main chain and π–π stacking in the substrate plane.[16] Contrary to this, a face-on orientation in the thin films with π–π stacking direction to the substrate normal improves the charge hopping in the out-of-plane direction, which is desirable for vertical/sandwich type devices like diodes and solar cells. The end-on orientation of the polymeric backbone has also been found to exhibit higher out-of-plane charge carrier mobility.[17,18,20,21]

Although the orientation of the CPs can also be controlled by the judicious molecular design; however, modifying the molecular structure affects the film crystallinity, concomitantly changing their physical properties. [7,22–24] Spin-coating, which is one of the commonly used method for thin fabrication in a variety of planer and sandwich devices lead to the formation of isotropic thin films with relatively lower crystallinity. At the same time, the use of conventional orientation methods like friction transfer and mechanical rubbing utilizing shear force to orient the CPs are not suitable for fabricating planer devices like OFETs owing to the dominant face-on molecular orientation.[16] Recently, the unidirectional floating film transfer method (UFTM) developed by us is a highly facile and cost-effective solution-processable method to prepare large-area, uniform and oriented thin films of CPs.[25–27] In UFTM, oriented and solid thin films are first prepared on an orthogonal liquid substrate, then transferred to the desired substrate. In a recent work, Syafutra et al.[28] demonstrated that the orientation in UFTM films is homogenous throughout the film thickness. These advantages allow us to use the UFTM films for any device geometry. In our earlier work, fabrication of multilayer thin films without any detrimental effect

on underlying layers has already been reported for FTM processed thin films, which is one of the intriguing issues for most of the thin film fabrication methods, especially using solution processing.[29]

There is considerable uncertainty about the effect of molecular orientation, such as edge-on and face-on, on the performance of planer and sandwich devices in thin films, owing to structural regioregularity, processing conditions, solvent nature, and pre-aggregation requirements, and reports vary from one study to another. [10,22,30–32] In such cases, it is difficult to pinpoint the explicit nature of the molecular orientation, when the intrinsic properties of polymer and crystallinity are also compromised. Therefore, in our present study, we have used two different kinds of poly (3-hexylthiophene) (P3HT) as the representative solution-processable CPs, one (RR-P3HT) with very high regioregularity of 99.5% and other as a non-regiocontrolled P3HT (NR-P3HT) having regioregularity of 65%. We prepared thin films of these CPs using UFTM and spin coating techniques to fabricate OFET as a planar device and OSD as a sandwich device to clarify the explicit role of molecular orientation on the device performances, as schematically shown in Fig. 1. Orientation and microstructural features in the thin films thus prepared were investigated by UV-visible absorption spectroscopy, atomic force microscopy (AFM), out-of-plane x-ray diffraction (XRD) and in-plane grazing incidence x-ray diffraction (GIXD). It has been clearly demonstrated that planar devices with edge-on-oriented films were much superior in comparison to devices with face-on oriented films. Interestingly, this trend was the opposite for sandwich devices, where more crystalline and edge-on oriented films prepared by UFTM exhibited inferior performance compared to devices utilizing thin films prepared by spin-coating with the mixed face-on and edge-on molecular orientations.

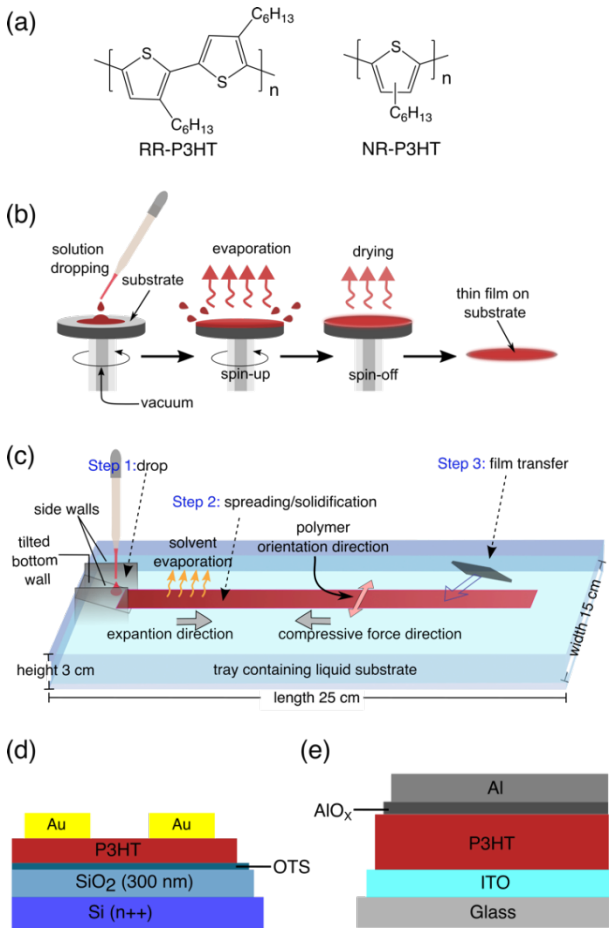

Figure 1. (a) Chemical structure of RR-P3HT and NR-P3HT. Schematic of the spin-coating process (b) and UFTM (c). Schematic of device structure OFET (d) and OSD (e). The polymer orientation direction in (c) was found to be perpendicular to the film expansion direction. OFETs were fabricated with polymer orientation direction parallel to the channel direction.

2. EXPERIMENTAL

2.1 Materials and Characterization

Electronic grade RR-P3HT and octadecyl(trichloro)silane (OTS), super dehydrated solvents (chloroform, toluene) were purchased from Sigma-Aldrich and used as received. NR-P3HT was synthesized in our laboratory by $FeCl_3$ mediated chemical oxidative polymerization as per our earlier publication and

purified by Soxhlet extraction sequentially by methanol and hexane for 12 hours each.[33] NMR characterization reveals its regioregularity to be 65%, while gel permeation chromatographic characterization indicated its number average molecular weight, weight average molecular weight and polydispersity index to be 110 kD, 28,811 kD and 3.83, respectively. Electronic absorption spectra of the films coated on the glass substrate were measured using a UV-visible-NIR spectrophotometer (JASCO V-570). A Glan−Thompson prism was placed between the sample and the incident light source for the polarized absorption spectral measurement. AFM images of the films were taken using a scanning probe microscope (JSPM, Shimadzu Japan). Thin films prepared on Si substrates were used for XRD and GIXD measurements, while for other optical characterization, glass substrates were used. The substrates were cleaned in ultrasonic baths of acetone, isopropanol, and chloroform (10 min each). Out-of-plane XRD measurements (θ−2θ scan) of the films were conducted using a Rigaku X-ray diffractometer with a Cu-Kα radiation source. Having an index of refraction less than unity, incident X-rays go through total external reflection while their grazing incident angle (ω) with the film surface is below the critical angle (ωc), i.e., ω <ωc. For in-plane GIXD measurements (φ−2θχ scan), the sample and the detector were rotated with angles of φ and 2θχ, respectively, while ω and scattered angle were fixed to 0.14° and 0.28°, respectively, from the sample surface. Additionally, the angle between film propagation during UFTM and the scattering vector (χ) was kept around 0° or 90° to probe anisotropy in the macromolecular arrangement of the thin film. On the other hand, the X-ray source and detector were rotated with the angles of θ and 2θ, respectively, from the sample surface for out-of-plane XRD measurement.

2.2 OSD Fabrication

For the fabrication of OSDs, ITO-coated glass was used as the substrate and making the Ohmic contact. Substrates were cleaned by using ultrasonic bath and solvents like toluene, acetone, methanol and 2-

propanol for 10 min. each. NR- and RR-P3HT were dissolved in chloroform (2% w/v) to fabricate thin films by spin coating and UFTM. Spin coated films were prepared at a spinning speed of 800 rpm for 10 s followed by 1500 rpm for 50 s to attain a film thickness of around 180 nm for both RR and NR P3HT. UFTM thin films were prepared placing a drop (10µl) of the polymer solution over the liquid substrate. The liquid substrate used was ethylene glycol and glycerol in the ratio of 3:1 at 50°C and cast onto the substrates. UFTM films of each CPs were coated six times by layer-by-layer coating for fabricating OSDs to achieve similar film thickness as spin-coated thin film as described in our earlier publication.[29] Later, these films were annealed at 120°C for 30 min under an argon glove box followed by slow cooling. Thermal evaporation of top metal pads under a high vacuum (~10^{-6} Torr) was carried out using the shadow masks with a cross-sectional area of 4 mm^2. The OSDs were fabricated with Al as top metal to form a Schottky barrier with AlO_X as the interlayer. To accomplish this, 10 nm of Al was first thermally evaporated on P3HT under high-vacuum, followed by exposing them to ambient conditions for ~ 1 hour to facilitate oxidation of Al to form AlO_X interlayer.[34] Then, 70 nm thick Al was thermally evaporated on AlO_X layer under high vacuum to complete the device fabrication.

2.3 OFET Fabrication

OFETs were fabricated on heavily p-doped Si substrate with 300 nm thermally grown SiO_2 as the dielectric layer with areal capacitance (C_i) of 10 nF/cm^2. All the substrates were subjected to the cleaning procedure described above in the section 2.2. Later, these substrates were subjected to RCA cleaning with batch 1 (DI water: concentrated ammonium hydroxide: H_2O_2 = 50:1:1) and batch 2 (DI water: concentrated HCl: H_2O_2 = 50:1:1) and cleaned with boiling ethanol at last. Substrates were then treated by emerging them in 20 mM OTS solution in chloroform for 36 h to form a self-assembled monolayer (SAM) on the SiO_2 surface. After SAM formation, the substrates were cleaned in an ultrasonic bath with chloroform for 10 min, and then substrates were annealed at 200°C for 30 min. The spin coated thin

films were prepared at a spinning speed of 2000 rpm for 60 s to attain a film thickness of around 80 nm for RR and 50 nm for NR P3HT. A single layer of UFTM thin films was fabricated under the same conditions as OSDs. These thin films were annealed at 120°C for 30 min under an argon glove box, followed by slow cooling. The film thickness for the single layer of NR and RR P3HT were around 25 nm and 30 nm. Later, source/drain electrodes were patterned using nickel shadow masks having channel length (*L*) and width (*W*) of 20 μm and 2 mm, respectively, by thermally evaporation of Gold (under ~ 10^{-6} Torr). Shadow mask was used in such a way that the polymer main-chain alignment direction lies in parallel to the channel length. The output and transfer characteristics of the OFETs were measured with a computer controlled two-channel source-measure unit (Keithley 2612).

3. RESULT AND DISCUSSION

3.1 Absorption Spectroscopy

Oriented and non-oriented (isotropic) thin films of RR-P3HT and NR-P3HT prepared by UFTM and spin coating techniques, respectively, were subjected to the optical characterization utilizing solid-state electronic absorption spectroscopy as shown in Fig. 2. The optical parameters of each film are given in Table 1. It can be seen from the solid-state absorption spectra of spin-coated RR-P3HT exhibiting absorption maximum (λ_{max}) at 514 nm along with well-discernible vibronic shoulders appearing at 550 nm and 600 nm (Fig. 2(a)). Well resolved vibronic shoulders in the spin coated thin films RR-P3HT indicate increased crystalline nature due to enhanced intermolecular interactions by facile lamellar π-π stacking.[35–38] On the other hand, spin coated thin films of the NR-P3HT exhibited slightly blue-shifted absorption spectral features with the λ_{max} at 508 nm and less-resolved vibronic shoulders at 544 nm and 594 nm. This blue-shifted spectral feature of NR-P3HT with less resolved shoulder associated with the 0-0 and 0-1 vibronic transitions is attributed to the decrease in the effective π-conjugation arising from coil-shaped twisted polymeric main chain due to the low regioregularity. [29,38] Unlike isotropic spin-

coated thin films, UFTM films exhibited anisotropic absorption spectra with a red-shift in the λ_{max} in the parallel-oriented thin films for RR-P3HT and NR-P3HT both. Molecular orientation estimated by the optical dichroic ratio (DR) clearly indicates that UFTM processed NR-P3HT thin films exhibited a much higher molecular orientation than RR-P3HT thin films.

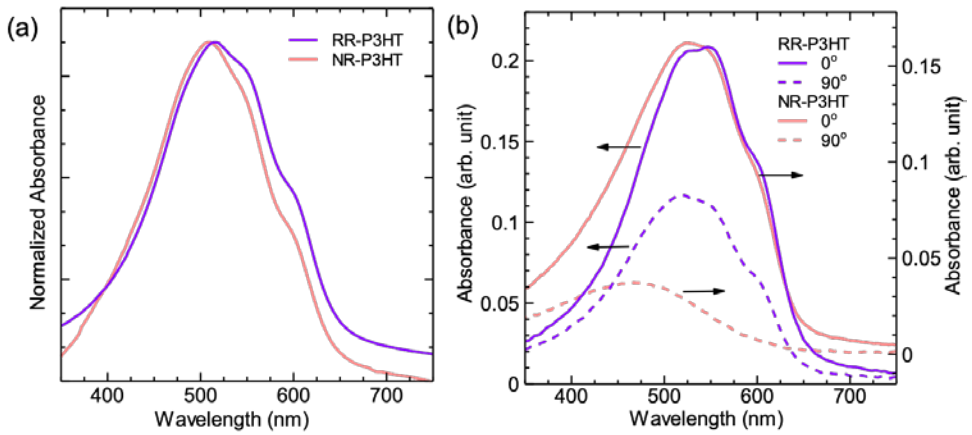

Figure 2. Normalized electronic absorption spectra of spin-coated thin films (a) and polarized absorption spectra of UFTM processed thin films (b) for RR-P3HT and NR-P3HT.

Table. 1. Optical parameters for isotropic spin-coated and anisotropic UFTM processed thin films of RR-and NR-P3HT fabricated on glass substrate.

	Film Preparation	Absorption maximum	Dichroic ratio	Vibronic shoulder
RR-P3HT	Spin coating	514 nm	-	550 nm, 600 nm
	UFTM parallel	528 nm	2.1	550 nm, 600 nm
	UFTM perpendicular	518 nm		550 nm, 600 nm-
NR-P3HT	Spin coating	508 nm		544 nm, 594 nm
	UFTM parallel	524 nm	6.2	548 nm, 598 nm
	UFTM perpendicular	480 nm		-

DR of the oriented RR-P3HT and NR-P3HT thin films prepared by UFTM were found to be 2.1 and 6.2, respectively. It should be noted that NR-P3HT exhibits high alignment tendency than RR-P3HT,

as reported in our earlier studies, where floating film fabrication was conducted in a conventional way using a petri-dish.[38,39] The low DR of the RR-P3HT is attributed to the high inter-digitation arising from the zipper effect due to the fish-bone-like structure.[40,41] The value of the λ_{max} for the parallel oriented films in the polarized absorption spectra of RR-P3HT and NR-P3HT is red-shifted by 14 and 16 nm, respectively, which is attributed to the increase in the effective π-conjugation due to the orientation of the polymeric backbone along the parallel direction. This red shift in RR-P3HT films is often attributed to the switching of the main-transition mode from 0–2 to 0–1 since this is well discussed in the past that the slow growth of the crystalline domain promoted the evolution of lower vibronic modes in RR-P3HT. As mentioned by Spano's model, the growth of 0–0 vibronic shoulder in RR-P3HT correlates the electronic structure of excitonic bandwidth with intermolecular coupling transition energy.[42,43] The less resolved absorption spectra of NR-P3HT compared to RR-P3HT can be attributed to an inhomogeneous broadening of the electronic π–π* transition caused by a relatively wider distribution of conjugation lengths. A careful perusal of the absorption spectra in perpendicular direction shows that RR-P3HT retains its vibronic features, and peak absorbance is blue-shifted only by 10 nm. On the other hand, perpendicular absorption spectra of the NR-P3HT are featureless, peak absorbance is blue-shifted by 44 nm, and it almost resembles the solution-state spectra of NR-P3HT. It can thus be explained by the fact that most of the macromolecules align along the orientation direction, and only a small portion of them fail to align and are randomly distributed or can be considered amorphous.

3.2 Thin Film Microstructural Characterization

3.2.1. AFM

To visualize the surface morphology of the NR- and RR-P3HT thin films prepared by spin coating and UFTM, AFM measurements were carried in tapping mode. AFM image in Fig. 3(a) shows

that spin-coated thin film of NR-P3HT is completely features less, demonstrating its isotropic and amorphous nature. Contrary to this, UFTM processed thin film of the same NR-P3HT exhibits clear and unidirectional alignment of polymeric domains in parallel to the polymer orientation direction, as shown in Fig. 3 (b). Therefore, combining the results of spectral features in (Fig. 2(b)) and AFM image (Fig. 3(b)), it can be concluded that UFTM not only improved film crystallinity but also promoted unidirectional alignment with large oriented micrometer-sized domains in the NR-P3HT. Contrary to the featureless surface morphology of the spin coated films of NR-P3HT, the spin-coated thin films of the RR-P3HT shown in Fig. 3(c) exhibited some structural features with isotropic morphology and very small (~200 nm) sized domains. However, UFTM processed oriented thin films of RR-P3HT shown in Fig. 3(d) exhibited well-oriented domains with sizes extending up to several micrometers in size that are well connected and these oriented domains were aligned in parallel to the polymer orientation direction.

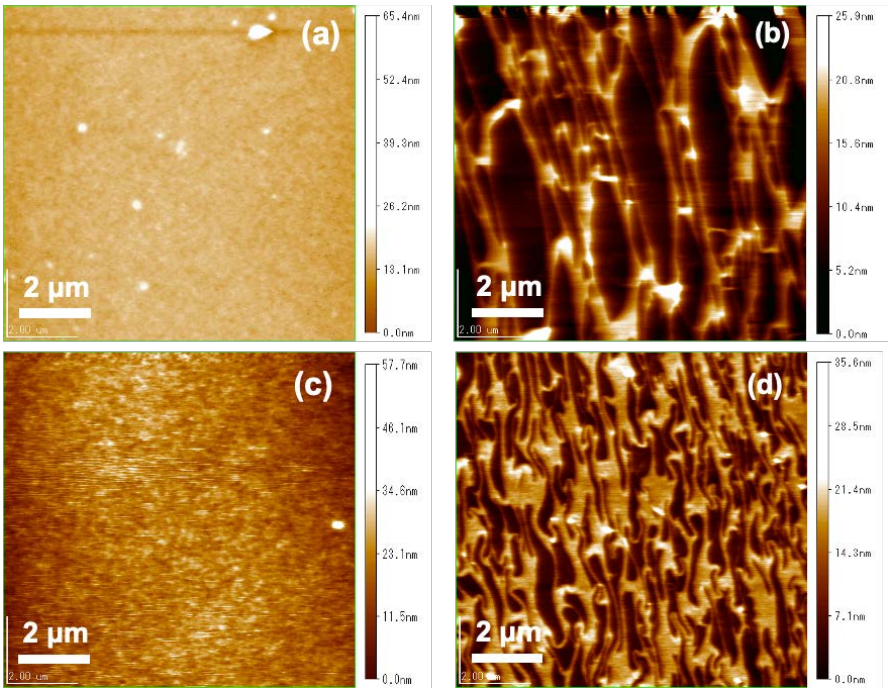

Figure 3. AFM height image of the films. NR-P3HT film prepared by spin coating (a) and UFTM (b). RR-P3HT film prepared by spin coating (c) and UFTM (d).

3.2.2. XRD

In order to examine the thin film crystallinity and visualize the macromolecular orientation, out-of-plane XRD and in-plane GIXD measurements were conducted following the method described in our earlier publications.[44,45] Out-of-plane XRD for the RR-P3HT films is shown in Fig. 4. RR-P3HT films prepared by UFTM exhibits a set of sharp diffraction peaks (h00) related to the lamellar stacking of the side-chains up to 3rd order at 5.33°, 10.65° and 15.99°. Contrary to this, its spin-coated thin film shows a relatively weak (h00) peak up to the 2nd order, which reflects that the films prepared by UFTM are more crystalline.

In-plane GIXD of RR-P3HT films is shown in Fig. 4 (b). RR-P3HT films prepared by UFTM exhibited no diffraction peaks associated with alkyl side chains, and only (0k0) diffraction peak related to the π–π stacking was observed at 23.2°, reflecting that all the crystallites are edge-on oriented.[9] It is interesting to see that spin-coated RR-P3HT film shows 100 and 0k0 diffraction peaks both, reflecting some fractions of crystallites in the films are face-on oriented too. Therefore, it can be concluded that spin-coated films used for present investigation have mixed edge-on and face-on oriented crystallites. In general, CPs adopt two types of possible macromolecular conformation in their thin-film that is edge-on, face-on (as illustrated in Fig. 4 (c and d)) or their mixed phases depending upon the selection of the conditions and parameters during thin film fabrication.

From out-of-plane and in-plane XRD profiles of the RR-P3HT thin films, it can be concluded that UFTM-prepared RR-P3HT films are more ordered and crystalline than spin-coated films. In the past, De Long champ et al. reported RR-P3HT/$CHCl_3$ spin-coated at spin speed ~2000 are preferentially face-on oriented,[30] and Yang et al. also reported that films P3HT/$CHCl_3$ yielded mostly face-on crystal orientation favorable for the vertical device.[10]

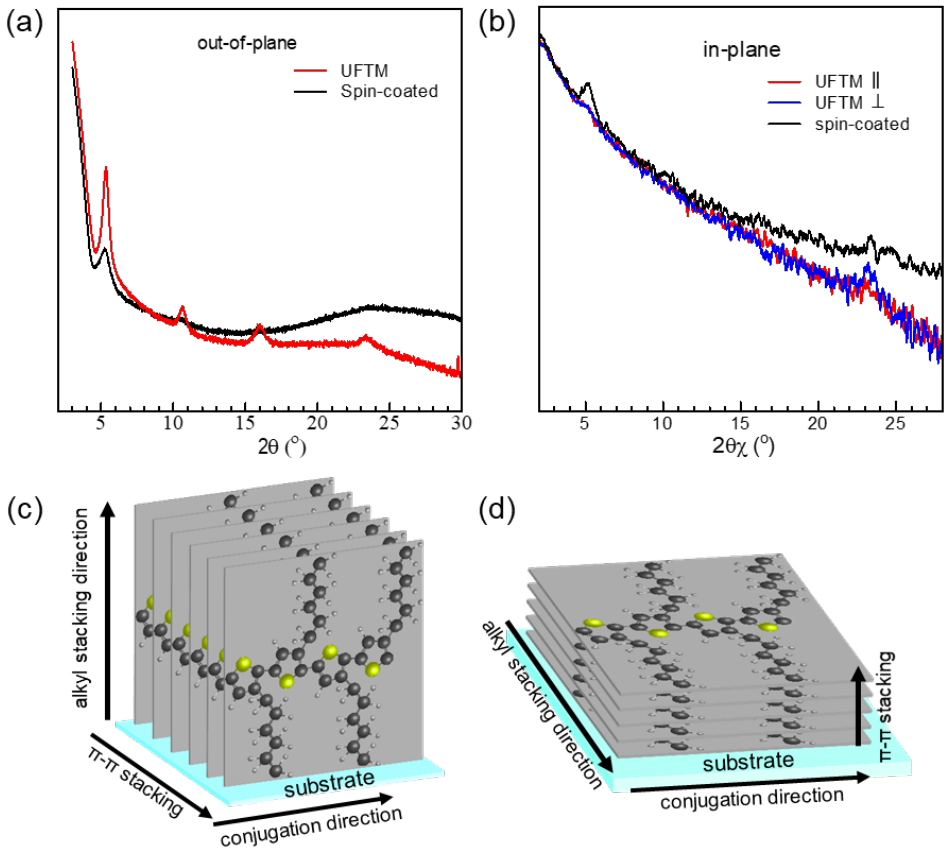

Figure 4. Out-of-plane (a) and in-plane (b) diffraction profiles of RR-P3HT films fabricated by spin-coating and UFTM. Schematic representation of edge-on (c) and face-on (d) orientations of P3HT with respect to substrate plane.

It is worth noticing that the low boiling point of chloroform or spinning facilitates the kinetically grown face-on oriented crystallites. However, when RR-P3HT film were prepared by spin-coating with a high boiling point solvent or using low spinning speeds, then polymers prefer to form thermodynamically favorable crystal structure for planar devices.[8,10,30] However, our earlier publications reported that floating films of the thiophene-based polymer generally adopt edge-on orientation.[9,46] X-ray diffraction results for NR-P3HT have already been reported in our earlier studies, where we found that the spin-coated and floating films were face-on and edge-on oriented, respectively.[29]

3.3 Device Characterization

3.3.1 OSD Performance

To examine the effect of molecular orientation in the out-of-plane charge transport, OSDs were fabricated utilizing the thin films of the RR-P3HT and NR-P3HT having purely edge-on and mixed edge-on/face-on orientations prepared by UFTM and spin coating techniques, respectively. The current density vs voltage (*J*-*V*) characteristics devices thus fabricated are shown in Fig 5, exhibiting typical asymmetric characteristics for OSDs. Electrical parameters deduced from the analysis of the *J*-*V* characteristics is summarized in table 2. This asymmetric J-V characteristic certainly manifests the facile current flow in the forward direction, while the current in the reverse direction is highly obstructed. This can be attributed to the formation of the Schottky barrier at the Al/AlO_x/P3HT interface. The thermionic emission model given in Equation (1), proposed for the inorganic Schottky diodes, has also been widely affirmed for the organic counterpart.[47–50]

$$J = J_0 \left[\exp\left(\frac{qV}{\eta kT}\right) - 1\right] \quad (1)$$

where

$$J_0 = A^* T^2 \exp\left(-\frac{q\phi_B}{\eta kT}\right) \quad (2)$$

Here, *J* and *V* represent current density and voltage, respectively. The constant terms are A^* is the Richardson constant, *k* is the Boltzmann constant, *T* is the absolute temperature, and *q* is the electric charge. Here device parameters η, J_0, and ϕ_B are ideality factor, reverse saturation current density and schottky barrier height, respectively. η and J_0 were calculated using the intercept and slope of the *J*-*V* plots. The rectification ratio (RR) was calculated from the ratio of current flowing under forward bias to the reverse bias at the same applied bias voltage.

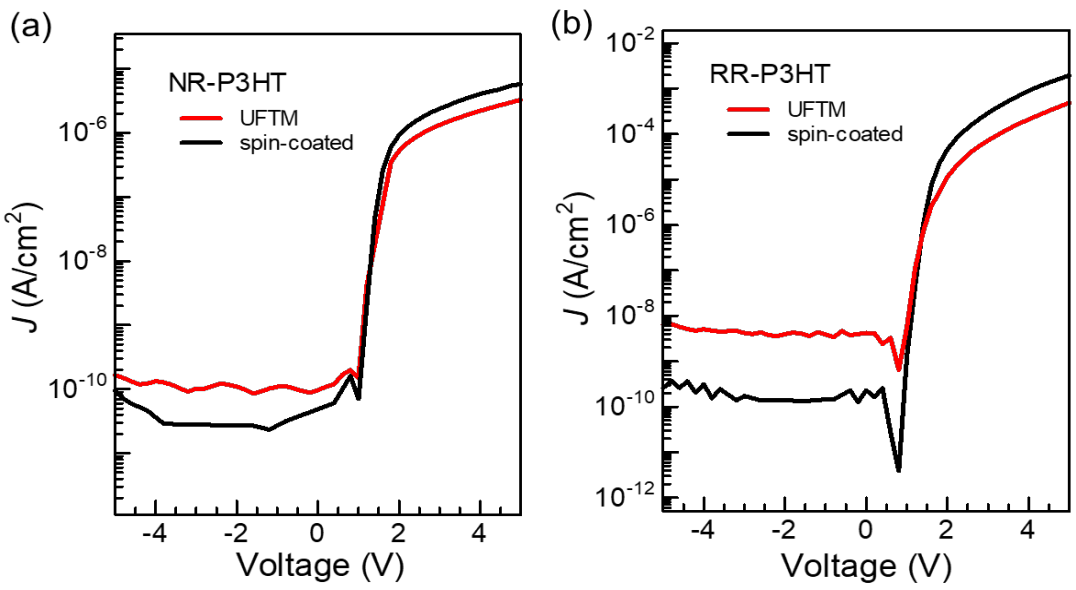

Figure 5. Current-voltage characteristics of organic Schottky diodes fabricated with UFTM films and spin-coated films of NR-P3HT (a) and RR-P3HT (b).

Table. 2. Electrical parameters deduced from the (*J*-*V*) characteristics of organic Schottky diodes fabricated using UFTM processed and spin-coated thin films of RR-P3HT and NR-P3HT. The values shown in parenthesis is the average values and standard deviations for 20 different independent devices.

Parameters	RR-P3HT (Spin Coated)	RR-P3HT (UFTM)	NR-P3HT (Spin-coated)	NR-P3HT (UFTM)
Rectification Ratio	8.7×10^6 ($5.8 \times 10^6 \pm 2.1\%$)	7.1×10^5 ($6.9 \times 10^5 \pm 4.6\%$)	8.2×10^4 ($7.7 \times 10^4 \pm 6.2\%$)	2.6×10^3 ($1.28 \times 10^3 \pm 7\%$)
Ideality Factor	2.11 (2.43 ± 3.6%)	3.45 (4.92 ± 3%)	2.5 (2.6 ± 5.1%)	3.57 (3.61 ± 2.4%)
Barrier Height	1.37 (1.38 ± 1%)	1.13 (1.15 ± 4%)	1.41 (1.45 ± 7%)	1.35 (1.36 ± 2.8%)

As shown in Fig. 5 and table 2, despite the high crystallinity and molecular ordering of UFTM films, spin coated films were far superior to UFTM films in OSDs prepared using both the CPs such as RR-P3HT or NR-P3HT. The RR for spin-coated thin films of NR-P3HT (8.2×10^4) was more than the UFTM coated thin films (2.6×10^3) by an order of magnitude. A similar trend was followed in the case of RR-P3HT films, where spin coated films had a much better RR (8.7×10^6) than the UFTM films (7.1×10^5). This clearly corroborates the dominant influence of molecular orientation controlling the out-of-

plane charge transport in ODSs, where edge-on oriented UFTM films with alkyl chain stacked normal to the substrate plane, hindering the vertical charge transport leading to the hampered device performance in OSDs. Irrespective of the methodology adopted for the fabrication of thin films to OSDs, devices based-on RR-P3HT exhibited better performance as compared to their NR-P3HT counterparts. The low performance of NR-P3HT could be attributed to its relatively higher number of defects than RR-P3HT.

3.3.1 OFET Performance

The effect of molecular orientation on controlling the device performance was further validated in planar devices also by fabricating OFETs. Output and transfer characteristics of OFETs for NR-P3HT and RR-P3HT films fabricated by the UFTM and spin coating are shown in Fig. 6. Note that channel direction was kept parallel to polymer main chain orientation direction for the UFTM films. Field-effect mobility (μ) was extracted from the transfer curves in the saturation region using the equation 3.

$$I_{DS} = \frac{\mu C_i W}{2L}(V_{GS} - V_{DS})^2 \qquad (3)$$

The μ was calculated by taking a slope of the $|I_{DS}|^{1/2} - V_{GS}$ plot in the saturated region. The on/off ratio was calculated by the ratio of on current and off current in the transfer characteristic. A clear p-type characteristic can be seen from the output characteristics (Fig. 6 (a and c)) in all of the OFETs. Output currents at a given applied gate voltage were enhanced by about two orders of magnitude in the films fabricated with UFTM for both of the NR-P3HT and RR-P3HT as compared to their corresponding spin-coated thin film-based device counterpart. Electronic parameters extracted from the transfer curves are summarized in the Table 3.

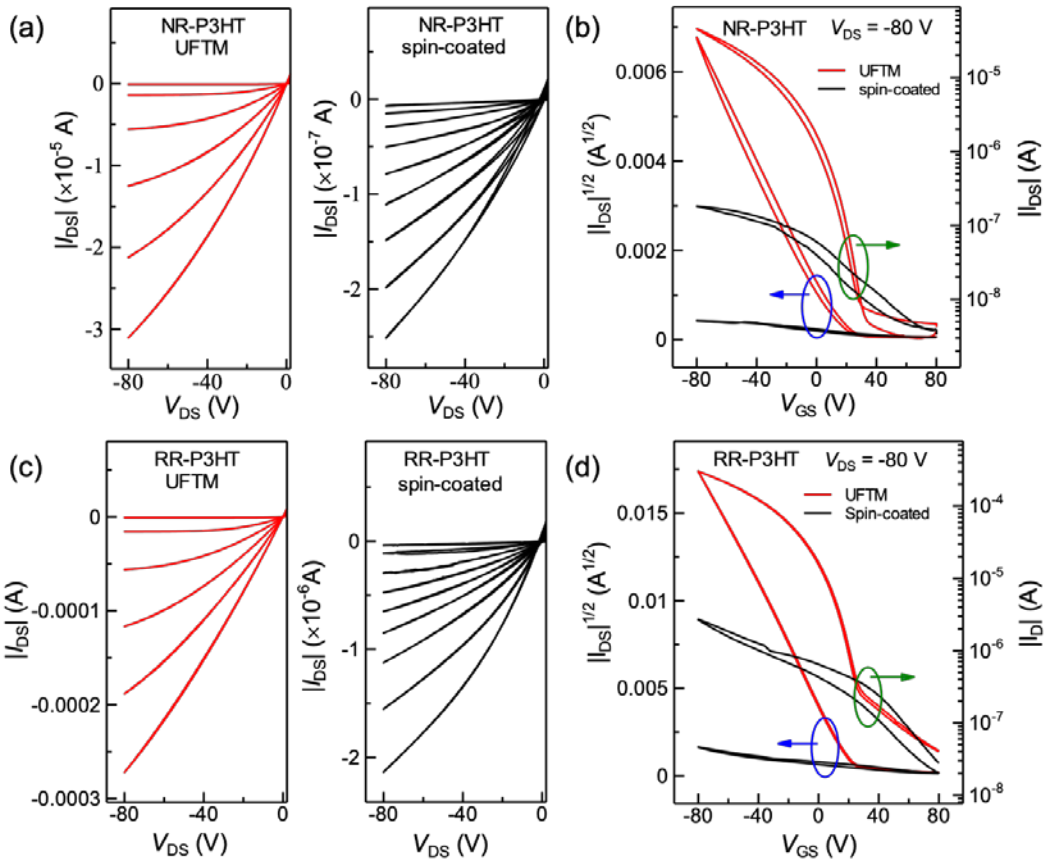

Figure 6. Output and transfer characteristics. (a, b) NR-P3HT films fabricated with UFTM and spin coating. (c, d) RR-P3HT films fabricated with UFTM and spin coating.

Table 3. Electronic parameters deduced from the OFETs characteristics fabricated using UFTM processed and spin coated thin films of RR-P3HT and NR-P3HT. Values shown in parenthesis exhibits the average values and standard deviations for 20 different independent devices.

Parameters	RR-P3HT (Spin-coating)	RR-P3HT (UFTM)	NR-P3HT (Spin-coating)	NR-P3HT (UFTM)
Mobility (cm^2/Vs)	7.2×10^{-4} ($6.1 \times 10^{-4} \pm 3.4\%$)	0.12 ($9.8 \times 10^{-2} \pm 2.1\%$)	4.1×10^{-5} ($2.9 \times 10^{-5} \pm 9\%$)	2.3×10^{-2} ($1.1 \times 10^{-2} \pm 2.7\%$)
on/off ratio	6.4×10^{2} ($5.5 \times 10^{2} \pm 2.6\%$)	1.2×10^{4} ($1.0 \times 10^{4} \pm 4.1\%$)	1.1×10^{2} ($1.0 \times 10^{2} \pm 3\%$)	2.4×10^{4} ($1.0 \times 10^{4} \pm 6.5\%$)

In the case of OFETs fabricated using NR-P3HT films prepared by UFTM, the μ estimated from the saturation region was found to be 2.3×10^{-2} cm^2/Vs ($I_{on}/I_{off} \approx 10^4$), which is about 3 orders of magnitude higher as compared to that of OFETs fabricated with spin-coated thin films counterparts having

estimated μ of 4.1×10^{-5} ($I_{on}/I_{off} \approx 10^2$). Demonstration of such a remarkable enhancement in μ in UFTM coated films of NR-P3HT in comparison to spin coated films is attributed to orientation of crystalline and edge-on domains with polymer oriented in the channel directions.

Presence of the face-on fractions with alkyl chains lying in the substrate plane in spin coated thin films leads to diminished planer charge transport resulting in to hampered OFET performance as compared to their UFTM processed device counterparts. Similar trend of enhanced planer charge transport for OFETs based-on UFTM films of RR-P3HTwas also observed demonstrating a higher average μ by more than 2 orders of magnitude (1.2×10^{-1} cm^2/Vs) as compared to that of OFETs utilizing spin coated thin films (7.2×10^{-4} cm^2/Vs). Enhanced crystallinity and favorable edge-on orientation led to remarkable enhancement in the OFETs with active layer films prepared by UFTM. RR-P3HT films prepared by UFTM have five-times higher μ than NR-P3HT films prepared by UFTM, which can be attributed to their relatively higher crystallinity and large fractions of crystalline domains as clearly confirmed by AFM (Fig. 3).

4. CONCLUSIONS

Large area oriented, anisotropic and non-oriented isotropic thin films of the RR-P3HT and NR-P3HT have been fabricated using the UFTM and spin coating, respectively. Thin Film characterization using electronic absorption spectroscopy reveals that UFTM films are more crystalline, oriented along with the enhanced intermolecular interactions in comparison to isotropic spin coated films. AFM images revealed that well connected micrometer sized domains aligned along orientation direction in comparison to featureless spin coated thin films. XRD and GIXD results clearly demonstrated that macromolecular chains in the UFTM films were purely edge-on oriented, whereas spin coated films have both face-on and edge-on oriented mixed phases. To probe the implication of nature of the

molecular orientation upon controlling the devices performance, OFETs and OSDs as representative devices for planer and vertical charge transport were fabricated using UFTM and spin-coated thin films, respectively. Despite of isotropic and less-crystalline spin coated films of RR-P3HT and NR P3HT as compared to their respective more crystalline and oriented UFTM films, OSDs based-on spin-coated thin films demonstrated superior device performance (enhanced RR, ideality factor and decreased barrier height) proving the importance of face-on orientation on the improved vertical. On the other hand, superior OFET performance for devices using UFTM films with remarkable enhancement ($>10^2$ times) in the μ as compared to their spin coated device counterparts pinpointed the significant contribution of the edge-on orientation of the thin films on controlling the in-plane charge transport. Therefore, it can be concluded that the nature of orientation of macromolecules has a profound impact on performance of the device under investigation, which is attributed to the differential nature of underlying charge transport responsible for the operation of the devices.

Conflict of Interest: The authors have no conflicts to disclose.

Acknowledgement: One of the authors, Shubham Sharma, would like to thank ministry of education, culture, sports, science and technology (MEXT) Japan for providing scholarship during his PhD program for the financial research, which is being gratefully acknowledged.

Funding: Authors declare no external funding.

REFERENCES:

(1) Sirringhaus, H. Device Physics of Solution-Processed Organic Field-Effect Transistors. *Adv. Mater.* **2005**, *17* (20), 2411–2425. https://doi.org/10.1002/adma.200501152.

(2) Sirringhaus, H. 25th Anniversary Article: Organic Field-Effect Transistors: The Path beyond Amorphous Silicon. *Adv. Mater.* **2014**, *26* (9), 1319–1335. https://doi.org/10.1002/adma.201304346.

(3) Oh, J. Y.; Rondeau-Gagné, S.; Chiu, Y. C.; Chortos, A.; Lissel, F.; Wang, G. J. N.; Schroeder, B. C.; Kurosawa, T.; Lopez, J.; Katsumata, T.; Xu, J.; Zhu, C.; Gu, X.; Bae, W. G.; Kim, Y.; Jin, L.; Chung, J. W.; Tok, J. B. H.; Bao, Z. Intrinsically Stretchable and Healable Semiconducting Polymer for Organic Transistors. *Nature* **2016**, *539* (7629), 411–415. https://doi.org/10.1038/nature20102.

(4) Xu, J.; Wu, H.-C.; Zhu, C.; Ehrlich, A.; Shaw, L.; Nikolka, M.; Wang, S.; Molina-Lopez, F.; Gu, X.; Luo, S.; Zhou, D.; Kim, Y.-H.; Wang, G.-J. N.; Gu, K.; Feig, V. R.; Chen, S.; Kim, Y.; Katsumata, T.; Zheng, Y.-Q.; Yan, H.; Chung, J. W.; Lopez, J.; Murmann, B.; Bao, Z. Multi-Scale Ordering in Highly Stretchable Polymer Semiconducting Films. *Nat. Mater.* **2019**, *18* (6), 594–601. https://doi.org/10.1038/s41563-019-0340-5.

(5) O'Connor, B. T.; Reid, O. G.; Zhang, X.; Kline, R. J.; Richter, L. J.; Gundlach, D. J.; Delongchamp, D. M.; Toney, M. F.; Kopidakis, N.; Rumbles, G. Morphological Origin of Charge Transport Anisotropy in Aligned Polythiophene Thin Films. *Adv. Funct. Mater.* **2014**, *24* (22), 3422–3431. https://doi.org/10.1002/adfm.201303351.

(6) Gurau, M. C.; Delongchamp, D. M.; Vogel, B. M.; Lin, E. K.; Fischer, D. A.; Sambasivan, S.; Richter, L. J. Measuring Molecular Order in Poly(3-Alkylthiophene) Thin Films with Polarizing Spectroscopies. *Langmuir* **2007**, *23* (2), 834–842. https://doi.org/10.1021/la0618972.

(7) Sirringhaus, H.; Brown, P. J.; Friend, R. H.; Nielsen, M. M.; Bechgaard, K.; Langeveld-Voss, B. M. W.; Spiering, a. J. H.; Janssen, R. a. J.; Meijer, E. W.; Herwig, P.; de Leeuw, D. M. Two-Dimensional Charge Transport in Self-Organized, High-Mobility Conjugated Polymers. *Nature* **1999**, *401* (6754), 685–688. https://doi.org/10.1038/44359.

(8) Chang, J. F.; Sun, B.; Breiby, D. W.; Nielsen, M. M.; Sölling, T. I.; Giles, M.; McCulloch, I.; Sirringhaus, H. Enhanced Mobility of Poly(3-Hexylthiophene) Transistors by Spin-Coating from High-Boiling-Point Solvents. *Chem. Mater.* **2004**, *16* (23), 4772–4776. https://doi.org/10.1021/cm049617w.

(9) Pandey, M.; Gowda, A.; Nagamatsu, S.; Kumar, S.; Takashima, W.; Hayase, S.; Pandey, S. S. Rapid Formation and Macroscopic Self-Assembly of Liquid-Crystalline, High-Mobility, Semiconducting Thienothiophene. *Adv. Mater. Interfaces* **2018**, *5* (6), 1700875. https://doi.org/10.1002/admi.201700875.

(10) Yang, H.; Lefevre, S. W.; Ryu, C. Y.; Bao, Z. Solubility-Driven Thin Film Structures of Regioregular Poly(3-Hexyl Thiophene) Using Volatile Solvents. *Appl. Phys. Lett.* **2007**, *90* (17), 172116. https://doi.org/10.1063/1.2734387.

(11) Soeda, J.; Matsui, H.; Okamoto, T.; Osaka, I.; Takimiya, K.; Takeya, J. Highly Oriented Polymer Semiconductor Films Compressed at the Surface of Ionic Liquids for High-Performance Polymeric Organic Field-Effect Transistors. *Adv. Mater.* **2014**, *26* (37), 6430–6435. https://doi.org/10.1002/adma.201401495.

(12) Zhao, F.; Wang, C.; Zhan, X. Morphology Control in Organic Solar Cells. *Adv. Energy Mater.* **2018**, *8* (28), 1703147. https://doi.org/10.1002/AENM.201703147.

(13) Osaka, I.; Takimiya, K. Backbone Orientation in Semiconducting Polymers. *Polymer (Guildf).* **2015**, *59*, A1–A15. https://doi.org/10.1016/j.polymer.2014.12.066.

(14) Kajiya, D.; Ozawa, S.; Koganezawa, T.; Saitow, K. I. Enhancement of Out-of-Plane Mobility in P3HT Film by Rubbing: Aggregation and Planarity Enhanced with Low Regioregularity. *J. Phys. Chem. C* **2015**, *119* (15), 7987–7995. https://doi.org/10.1021/jp510675r.

(15) Tremel, K.; Ludwigs, S. Morphology of P3HT in Thin Films in Relation to Optical and Electrical Properties. In *P3HT Revisited - From Molecular Scale to Solar Cell Devices From Molecular Scale to Solar Cell Devices*; Ludwigs, S., Ed.; Springer Berlin Heidelberg, 2012; pp 39–82. https://doi.org/10.1007/12_2014_288.

(16) Pandey, M.; Kumari, N.; Nagamatsu, S.; Pandey, S. S. Recent Advances in the Orientation of Conjugated Polymers for Organic Field-Effect Transistors. *J. Mater. Chem. C* **2019**, *7* (43), 13323–13351. https://doi.org/10.1039/c9tc04397g.

(17) Hashimoto, K.; Koganezawa, T.; Tajima, K. End-On Orientation of Semiconducting Polymers in Thin Films Induced by Surface Segregation of Fluoroalkyl Chains. *J. Am. Chem. Soc.* **2013**, *135* (26), 9644–9647.

(18) Ma, J.; Hashimoto, K.; Koganezawa, T.; Tajima, K. Enhanced Vertical Carrier Mobility in Poly (3- Alkylthiophene) Thin Films Sandwiched between Self-Assembled Monolayers and Surface- Segregated Layers. *Chem. Commun.* **2014**, *50* (27), 3627. https://doi.org/10.1039/c3cc49760g.

(19) Wang, F.; Hashimoto, K.; Segawa, H.; Tajima, K. Effects of Chain Orientation in Self-Organized Buffer Layers Based on Poly(3-Alkylthiophene)s for Organic Photovoltaics. *ACS Appl. Mater. Interfaces* **2018**, *10* (10), 8901–8908.

(20) Skrypnychuk, V.; Boulanger, N.; Yu, V.; Hilke, M.; Mannsfeld, S. C. B.; Toney, M. F.; Barbero. Enhanced Vertical Charge Transport in a Semiconducting P3ht Thin Film on Single Layer Graphene. *Adv. Funct. Mater.* **2015**, *25* (5), 664–670. https://doi.org/10.1002/adfm.201403418.

(21) Skrypnychuk, V.; Wetzelaer, G. J. A. H.; Gordiichuk, P. I.; Mannsfeld, S. C. B.; Herrmann, A.; Toney, M. F.; Barbero, D. R. Ultrahigh Mobility in an Organic Semiconductor by Vertical Chain Alignment. *Adv. Mater.* **2016**, *28* (12), 2359–2366. https://doi.org/10.1002/adma.201503422.

(22) Steyrleuthner, R.; Di Pietro, R.; Collins, B. A.; Polzer, F.; Himmelberger, S.; Schubert, M.; Chen, Z.; Zhang, S.; Salleo, A.; Ade, H.; Facchetti, A.; Neher, D. The Role of Regioregularity, Crystallinity, and Chain Orientation on Electron Transport in a High-Mobility n-Type Copolymer. *J. Am. Chem. Soc.* **2014**, *136* (11), 4245–4256. https://doi.org/10.1021/ja4118736.

(23) Wang, W.-C.; Chen, S.-Y.; Yang, Y.-W.; Hsu, C.-S.; Tajima, K. Face-on Reorientation of π-Conjugated Polymers in Thin Films by Surface-Segregated Monolayers. *J. Mater. Chem. A* **2020**, *8* (13), 6268–6275. https://doi.org/10.1039/D0TA00030B.

(24) Biniek, L.; Schroeder, B. C.; Nielsen, C. B.; McCulloch, I. Recent Advances in High Mobility Donor–Acceptor Semiconducting Polymers. *J. Mater. Chem.* **2012**, *22* (30), 14803. https://doi.org/10.1039/c2jm31943h.

(25) Pandey, M.; Syafutra, H.; Kumari, N.; Pandey, S. S.; Abe, R.; Benten, H.; Nakamura, M. Extreme Orientational Uniformity in Large-Area Floating Films of Semiconducting Polymers for Their Application in Flexible Electronics. *ACS Appl. Mater. Interfaces* **2021**, *13* (32), 38534–38543. https://doi.org/10.1021/acsami.1c09671.

(26) Tripathi, A. S. M.; Pandey, M.; Sadakata, S.; Nagamatsu, S.; Takashima, W.; Hayase, S.; Pandey, S. S. Anisotropic Charge Transport in Highly Oriented Films of Semiconducting Polymer Prepared by Ribbon-Shaped Floating Film. *Appl. Phys. Lett.* **2018**, *112* (12), 123301. https://doi.org/10.1063/1.5000566.

(27) Pandey, M.; Singh, V.; Kumar, C.; Pandey, S. S.; Nakamura, M. Recent Progress in the Macroscopic Orientation of Semiconducting Polymers by Floating Film Transfer Method. *Jpn. J. Appl. Phys.* **2022**, *61*, SB0801. https://doi.org/10.35848/1347-4065/AC2F20.

(28) Syafutra, H.; Toyoda, J.; Pandey, M.; Kumari, N.; Benten, H.; Nakamura, M. Perfectness of the Main-Chain Alignment in the Conjugated Polymer Films Prepared by the Floating Film Transfer Method. *Appl. Phys. Lett.* **2022**, *120* (20), 203301. https://doi.org/10.1063/5.0088011.

(29) Pandey, M.; Sadakata, S.; Nagamatsu, S.; Pandey, S. S. S.; Hayase, S.; Takashima, W. Layer-by-Layer Coating of Oriented Conjugated Polymer Films towards Anisotropic Electronics. *Synth. Met.* **2017**, *227*, 29–36.

https://doi.org/10.1016/j.synthmet.2017.02.018.

(30) DeLongchamp, D. M.; Vogel, B. M.; Jung, Y.; Gurau, M. C.; Richter, C. A.; Kirillov, O. A.; Obrzut, J.; Fischer, D. A.; Sambasivan, S.; Richter, L. J.; Lin, E. K. Variations in Semiconducting Polymer Microstructure and Hole Mobility with Spin-Coating Speed. *Chem. Mater.* **2005**, *17* (23), 5610–5612. https://doi.org/10.1021/cm0513637.

(31) Rivnay, J.; Steyrleuthner, R.; Jimison, L. H.; Casadei, A.; Chen, Z.; Toney, M. F.; Facchetti, A.; Neher, D.; Salleo, A. Drastic Control of Texture in a High Performance N-Type Polymeric Semiconductor and Implications for Charge Transport. *Macromolecules* **2011**, *44* (13), 5246–5255. https://doi.org/10.1021/MA200864S.

(32) Biniek, L.; Leclerc, N.; Heiser, T.; Bechara, R.; Brinkmann, M. Large Scale Alignment and Charge Transport Anisotropy of PBTTT Films Oriented by High Temperature Rubbing. *Macromolecules* **2013**, *46* (10), 4014–4023. https://doi.org/10.1021/ma400516d.

(33) Pandey, S. S.; Takashima, W.; Nagamatsu, S.; Kaneto, K. Effect of Synthetic Impurities on Photocarrier Transport in Poly (3-Hexylthiophene). *IEICE Trans. Electron.* **2000**, *39* (7), 1088–1093.

(34) Kumari, N.; Pandey, M.; Hamada, K.; Hirotani, D.; Nagamatsu, S.; Hayase, S.; Pandey, S. S. Role of Device Architecture and AlO<inf>X</Inf> Interlayer in Organic Schottky Diodes and Their Interpretation by Analytical Modeling. *J. Appl. Phys.* **2019**, *126* (12). https://doi.org/10.1063/1.5109083.

(35) Brown, P.; Thomas, D.; Köhler, A.; Wilson, J.; Kim, J.-S.; Ramsdale, C.; Sirringhaus, H.; Friend, R. Effect of Interchain Interactions on the Absorption and Emission of Poly(3-Hexylthiophene). *Phys. Rev. B* **2003**, *67* (6), 1–16. https://doi.org/10.1103/PhysRevB.67.064203.

(36) Brinkmann, M. Structure and Morphology Control in Thin Films of Regioregular Poly(3-Hexylthiophene). *J. Polym. Sci. Part B Polym. Phys.* **2011**, *49* (17), 1218–1233. https://doi.org/10.1002/polb.22310.

(37) Morita, T.; Singh, V.; Nagamatsu, S.; Oku, S.; Takashima, W.; Kaneto, K. Enhancement of Transport Characteristics in Poly(3-Hexylthiophene) Films Deposited with Floating Film Transfer Method. *Appl. Phys. Express* **2009**, *2* (11), 111502. https://doi.org/10.1143/apex.2.111502.

(38) Pandey, M.; Nagamatsu, S.; Pandey, S. S. S.; Hayase, S.; Takashima, W. Enhancement of Carrier Mobility along with Anisotropic Transport in Non-

Regiocontrolled Poly (3-Hexylthiophene) Films Processed by Floating Film Transfer Method. *Org. Electron.* **2016**, *38*, 115–120. https://doi.org/10.1016/j.orgel.2016.08.003.

(39) Pandey, M.; Nagamatsu, S.; Pandey, S. S. S.; Hayase, S.; Takashima, W. Orientation Characteristics of Non-Regiocontrolled Poly (3-Hexyl-Thiophene) Film by FTM on Various Liquid Substrates. *J. Phys. Conf. Ser.* **2016**, *704* (1), 012005. https://doi.org/10.1088/1742-6596/704/1/012005.

(40) Yang, C.; Orfino, F. P.; Holdcroft, S. A Phenomenological Model for Predicting Thermochromism of Regioregular and Nonregioregular Poly(3-Alkylthiophenes). *Macromolecules* **1996**, *29* (20), 6510–6517. https://doi.org/10.1021/ma9604799.

(41) Tashiro, K.; Ono, K.; Minagawa, Y.; Kobayashi, M.; Kawai, T.; Yoshino, K. Structure and Thermochromic Solid State-Phase Transition of Poly (3-Alkylthiophene). *J. Polym. Sci. Part B Polym. Phys.* **1991**, *29* (10), 1223–1233. https://doi.org/10.1002/polb.1991.090291007.

(42) Spano, F. C. Modeling Disorder in Polymer Aggregates: The Optical Spectroscopy of Regioregular Poly(3-Hexylthiophene) Thin Films. *J. Chem. Phys.* **2005**, *122* (23), 234701. https://doi.org/10.1063/1.1914768.

(43) Pandey, M.; Nagamatsu, S.; Takashima, W.; Pandey, S. S.; Hayase, S. Interplay of Orientation and Blending: Synergistic Enhancement of Field Effect Mobility in Thiophene-Based Conjugated Polymers. *J. Phys. Chem. C* **2017**, *121* (21), 11184–11193. https://doi.org/10.1021/acs.jpcc.7b03416.

(44) Kumari, N.; Pandey, M.; Nagamatsu, S.; Nakamura, M.; Pandey, S. S. Investigation and Control of Charge Transport Anisotropy in Highly Oriented Friction-Transferred Polythiophene Thin Films. **2020**, *12* (10), 11876–11883. https://doi.org/10.1021/acsami.9b23345.

(45) Nagamatsu, S.; Misaki, M.; Chikamatsu, M.; Kimura, T.; Yoshida, Y.; Azumi, R.; Tanigaki, N.; Yase, K. Crystal Structure of Friction-Transferred Poly(2,5-Dioctyloxy-1,4-Phenylenevinylene). *J. Phys. Chem. B* **2007**, *111* (17), 4349–4354. https://doi.org/10.1021/jp067555m.

(46) Pandey, M.; Pandey, S. S.; Nagamatsu, S.; Hayase, S.; Takashima, W. Solvent Driven Performance in Thin Floating-Films of PBTTT for Organic Field Effect Transistor: Role of Macroscopic Orientation. *Org. Electron.* **2017**, *43*, 240–246. https://doi.org/10.1016/j.orgel.2017.01.031.

(47) Sze, S. M.; Ng, K. K. *Physics of Semiconductor Devices*, 3rd ed.; John Wiley & Sons, Inc., 2006. https://doi.org/10.1002/0470068329.

(48) Kaneto, K.; Takashima, W. Fabrication and Characteristics of Schottky Diodes Based on Regioregular Poly(3-Hexylthiophene)/Al Junction. *Curr. Appl. Phys.* **2001**, *1* (4–5), 355–361. https://doi.org/10.1016/S1567-1739(01)00035-9.

(49) Güllü, O.; Aydoğan, S.; Türüt, A. High Barrier Schottky Diode with Organic Interlayer. *Solid State Commun.* **2012**, *152* (5), 381–385. https://doi.org/10.1016/J.SSC.2011.12.007.

(50) Gunduz, B.; Yahia, I. S.; Yakuphanoglu, F. Electrical and Photoconductivity Properties of P-Si/P3HT/Al and p-Si/P3HT:MEH-PPV/Al Organic Devices: Comparison Study. *Microelectron. Eng.* **2012**, *98*, 41–57. https://doi.org/10.1016/J.MEE.2012.06.003.